*The Journal of Experimental Biology* **198**, 1809–1815 (1995)
Printed in Great Britain © The Company of Biologists Limited 1995



# THE MODE OF ATP-DEPENDENT MICROTUBULE–KINESIN SLIDING IN THE AUXOTONIC CONDITION

I. SHIRAKAWA[1], K. OIWA[1,*], S. CHAEN[1], T. SHIMIZU[2], H. TANAKA[1] AND H. SUGI[1,†]

[1]*Department of Physiology, School of Medicine, Teikyo University, Itabashi-ku, Tokyo 173, Japan* and
[2]*National Institute of Bioscience and Human Technology, Tsukuba, Ibaraki 305, Japan*

*Accepted 5 May 1995*

## Summary

**Kinesin is a motor protein that converts chemical energy derived from ATP hydrolysis into mechanical work to transport cellular components along microtubules. We studied the properties of ATP-dependent microtubule–kinesin sliding with two different *in vitro* assay systems. In one assay system, a kinesin-coated glass microneedle (elastic coefficient, 1–2.5 pN $\mu m^{-1}$) was made to slide along an axoneme. Using this system, we obtained the relationship between the force (=load) on the microneedle and the velocity of microneedle–kinesin sliding in the auxotonic condition, in which the load on the microtubule–kinesin contacts increased as sliding progressed. The force–velocity curve was upwardly convex (maximum velocity $V_{max}$, 0.58±0.15 $\mu m\,s^{-1}$; maximum isometric force $P_0$, 5.0±1.6 pN) and was similar to that of *in vitro* actin–myosin sliding in the auxotonic condition, suggesting that the two motor protein systems have fundamental kinetic properties in common. In the other assay system, an axoneme attached to a glass microneedle (elastic coefficient, 4–5 pN $\mu m^{-1}$) was made to slide on a kinesin-coated glass surface ($V_{max}$, 0.68±0.17 $\mu m\,s^{-1}$; $P_0$, 46.1±18.6 pN). The change in shape of the axoneme indicated an enormous flexibility of randomly oriented kinesin molecules.**

Key words: microtubule–kinesin sliding, auxotonic condition, force–velocity relationship, *in vitro* motility assay.

## Introduction

Myosin, dynein and kinesin are motor proteins that have the ability to convert chemical energy derived from ATP hydrolysis into mechanical work. The chemomechanical energy conversion is associated with a cyclic reaction between a motor protein molecule and a cytoskeletal polymer; an actin filament for myosin and a microtubule for dynein and kinesin. This cyclic reaction is coupled with ATP hydrolysis and is believed to consist of binding of the motor protein to the polymer, a conformational change of the motor protein producing the motor protein–polymer sliding, followed by detachment of the motor protein from the polymer before rebinding to another site along the polymer to initiate another cycle. Although extensive studies have been carried out on the enzyme kinetics of these motor protein systems, how the ATPase reaction steps are related to the motor protein–polymer sliding remains unknown.

To elucidate the mechanisms of these motor protein functions at the molecular level, various *in vitro* motility assay systems have been developed, with which it is now possible to obtain information about the relationship between force and velocity during actin–myosin sliding (Chaen *et al.* 1989; Oiwa *et al.* 1990) and during microtubule–kinesin sliding (Hall *et al.* 1993; Hunt *et al.* 1994; Svoboda and Block, 1994). Concerning microtubule–kinesin sliding, the attention of investigators tends to be focused on the behaviour of single kinesin molecules. We are of the opinion, however, that the behaviour of more than one kinesin molecule, including functional cooperativity among them, is at least as important as that of single molecules, since the normal cellular function of kinesin is believed to involve more than one molecule.

Based on this viewpoint, the present work was undertaken to study the mode of microtubule–kinesin sliding using two different *in vitro* assay systems; in one system, a kinesin-coated glass microneedle was made to slide along an axoneme, while in the other assay system, an axoneme-attached microneedle was made to slide on a kinesin-coated glass surface. In both cases, the force (=load) on the microtubule–kinesin contact increased as the degree of microneedle bending increased, to provide an auxotonic condition in which the load increases linearly as sliding

*Present address: Biological Function Section, KARC Communications Research Laboratory, Nishi-ku, Kobe 651-24, Japan.
†Author for correspondence.

progresses. It will be shown that the shape of the force–velocity relationship obtained with the former system was upwardly convex, as was the case for actin–myosin sliding under the auxotonic condition (Chaen *et al.* 1989), and that there is a functional cooperativity among randomly oriented kinesin molecules.

## Materials and methods

### *Preparation of kinesin*

Kinesin was purified according to the method described by Shimizu *et al.* (1991) with slight modifications. Briefly, a high-speed (approximately 100 000 ***g***) supernatant of bovine brain homogenate was kept at 37 °C for 30 min in the presence of 33 % glycerol and 1 mmol $l^{-1}$ ATP to polymerize microtubules. Then, apyrase (0.5 i.u. $ml^{-1}$, Sigma A6132) and 5′-adenylylimidodiphosphate (AMPPNP) (50 $\mu$mol $l^{-1}$) were added to the sample to deplete nucleoside triphosphates and to induce binding of kinesin to microtubules. Microtubules pelleted by centrifugation (at approximately 100 000 ***g***) were then incubated with 5 mmol $l^{-1}$ MgATP to release kinesin from the microtubules. Kinesin was purified with phosphocellulose P11 (Whatman) and DEAE–Sephacel (Pharmacia) column chromatography followed by sucrose density gradient sedimentation (5 % to 20 % sucrose in 100 mmol $l^{-1}$ Pipes, 2 mmol $l^{-1}$ $MgCl_2$, 1 mmol $l^{-1}$ EGTA, 0.5 mmol $l^{-1}$ dithiothreitol; pH 6.8). The collected fraction (kinesin solution), containing 60–110 $\mu$g $ml^{-1}$ kinesin as measured by the method of Bradford (1976), was stored at −80 °C.

### *Preparation of axonemes*

Living sea-urchin (*Hemicentrotus pulcherrimus* or *Clypeaster japonicus*) spermatozoa were suspended in a 20 % sucrose solution (at 4 °C) and homogenized to cause osmotic rupture. The homogenate was then subjected to differential centrifugation to obtain the axonemes free of sperm heads and membrane fragments (Bell *et al.* 1982). In some cases, the spermatozoa were demembranated by treatment with 0.04 % Triton X-100 to obtain axonemes to which the sperm heads remained attached. After the removal of dynein from the axonemes by incubation in a high-salt solution (0.6 mol $l^{-1}$ NaCl, 4 mmol $l^{-1}$ $MgSO_4$, 1 mmol $l^{-1}$ $CaCl_2$, 1 mmol $l^{-1}$ EDTA, 1 mmol $l^{-1}$ dithiothreitol, 10 mmol $l^{-1}$ Pipes; pH 7.0), the axonemes were resuspended in a solution containing 50 mmol $l^{-1}$ KCl, 2 mmol $l^{-1}$ $MgCl_2$, 1 mmol $l^{-1}$ EGTA, 0.5 mmol $l^{-1}$ dithiothreitol, 80 mmol $l^{-1}$ Pipes, pH 6.8 (axoneme solution), and stored at −80 °C.

### *Calibration of the glass microneedle*

Glass microneedles (tip diameter, 1–2 $\mu$m) were made from glass rods (diameter, 1 mm) with a microelectrode puller (Narishige, PD-5) in two steps: (1) the middle of a needle was pulled to reduce the diameter to about 0.1 mm; and (2) this part was further pulled to obtain two separate microneedles. The proximal part of the microneedle tapered sharply so that the needle diameter was reduced from 1 mm to about 10 $\mu$m over 3–4 mm along the needle length, while the distal part tapered less sharply so that the diameter was reduced from 10 to 1–2 $\mu$m over 2–3 mm. The elastic coefficient of the microneedles was determined using the method of Yoneda (1960). First, the compliance of a relatively rigid glass needle (reference needle; elastic coefficient, 16.3 nN $\mu m^{-1}$) was determined by adding a known weight to its tip and measuring the tip bending using a microscope. Then, the compliance of another, less-rigid needle (elastic coefficient, 2.27–3.81 nN $\mu m^{-1}$) was determined by pushing it against the reference needle. By repeating the above procedure three further times (elastic coefficient of the reference needles, 242–401, 30–92 and 5.6–14.4 pN $\mu m^{-1}$, respectively), the elastic coefficient of the microneedle used in the present experiments was determined with an overall accuracy of ±15 %.

### *Experimental arrangement*

Fig. 1 shows the experimental arrangement for the two *in vitro* assay systems, which will hereafter be called assay systems A and B. Both assay systems consisted of a glass slide mounted on the mechanical stage of an inverted microscope (Zeiss, Axiovert 35), a pair of Lucite blocks constituting the side walls of the chamber and a glass plate constituting the upper wall of the chamber. The surface of the glass slide, i.e. the bottom of the chamber, was covered by axonemes adsorbed onto the glass surface (see below) in assay system A (Fig. 1A) or coated with kinesin molecules in assay system B (Fig. 1B). A glass coverslip (4.5 mm×18 mm) was placed on the bottom of the chamber so that it was separated from the chamber by approximately 100 $\mu$m with greased slivers of coverslip. Axoneme solution (10 $\mu$l, assay system A) or 10 $\mu$l of kinesin solution (30 $\mu$g $ml^{-1}$, assay system B) was introduced into the space between the coverslip and the chamber. After 5 min, the coverslip was removed from the chamber, and the chamber was filled with the experimental solution containing 50 mmol $l^{-1}$ KCl, 2 mmol $l^{-1}$ $MgCl_2$, 1 mmol $l^{-1}$ EGTA, 2 mmol $l^{-1}$ ATP, 0.5 mmol $l^{-1}$ dithiothreitol and 80 mmol $l^{-1}$ Pipes (pH 6.8).

### *Experimental procedure and recording*

In assay system A, a glass microneedle (elastic coefficient, 1–2.5 pN $\mu m^{-1}$) was coated with kinesin by immersing its tip in a 10 $\mu$l drop of kinesin solution (100 $\mu$g $ml^{-1}$) for 5 min and then inserted into the experimental chamber filled with the experimental solution using a hydraulic micromanipulator (Narishige, WR-88L). The angle between the needle and the plane of the chamber was 10–15 °. The kinesin-coated tip of the microneedle was brought into contact with an axoneme adsorbed onto the bottom of the chamber with its long axis at right angles to the microneedle (see Fig. 2). In assay system B, a glass microneedle (elastic coefficient, 4–5 pN $\mu m^{-1}$) was first coated with poly L-lysine by immersing its tip in a solution containing poly L-lysine (10 mg $ml^{-1}$) and was then inserted into the experimental chamber filled with the experimental

solution (using the micromanipulator). Axonemes suspended in the axoneme solution were sprayed onto the needle tip with a microinjection device consisting of a hand-operated syringe and a glass micropipette (diameter, approximately 30 $\mu$m). Using this procedure, a microneedle with a single axoneme attached near its tip could be obtained (see Fig. 5).

In both assay systems, ATP-dependent microneedle movement was observed under Nomarski differential contrast (Zeiss 40× dry objective, numerical aperture 0.55) and recorded using a video camera (Hamamatsu, C 2400-77; 30 frames $s^{-1}$) connected to a video cassette recorder (Panasonic, AG-7355). Analysis of the movement was carried out using the same video casette recorder. Changes in the position of the microneedle were measured on the monitor screen (magnification, ×4250) using an image processor (Hamamatsu, Argus 10). The resolution was 80 nm.

All experiments were performed at room temperature (23–26 °C).

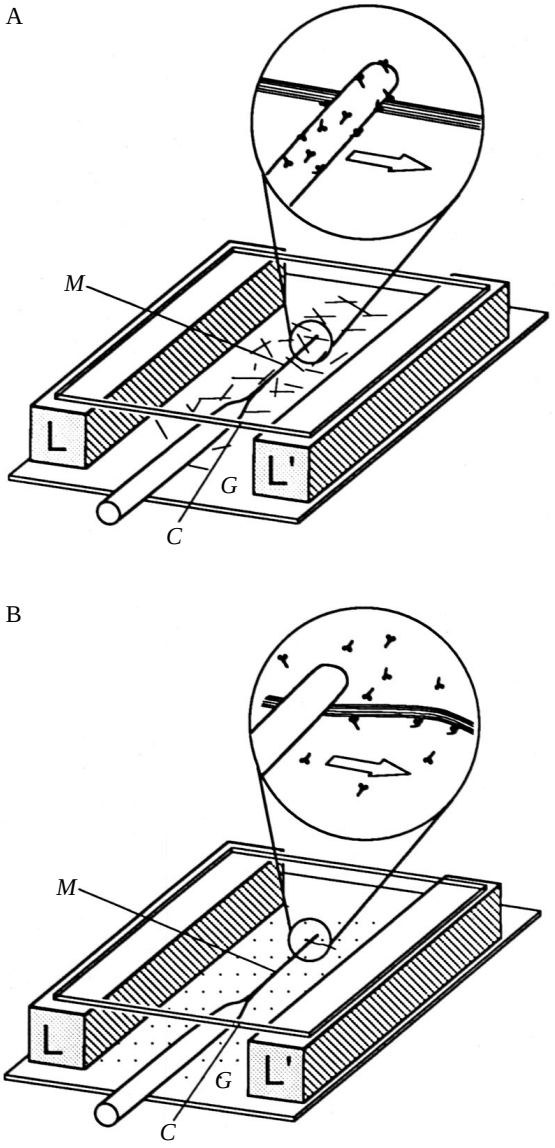


Fig. 1. Diagrams showing the two different assay systems used in the present study. (A) Assay system A. The kinesin-coated glass microneedle (*M*) was made to slide on an axoneme attached to the glass surface (*G*). (B) Assay system B. An axoneme attached to the glass microneedle (*M*) was made to slide on the kinesin-coated glass surface (*G*). L and L′ are Lucite blocks, 2 mm high, supporting the glass plate (*C*, 1.5 cm×2.5 cm) that formed upper surface of the chamber. For further explanation, see text.

## Results

### *Movement of the kinesin-coated microneedle along the axoneme*

#### *General features of the microneedle movement*

Fig. 2 shows selected frames from a video tape showing a kinesin-coated microneedle moving along an axoneme with its long axis oriented at right angles to the microneedle. As soon as the needle tip was brought into contact with the axoneme, it began to move along the axoneme in one direction over a distance of 2–10 $\mu$m. It eventually stopped after 5–30 s when the forces generated by the microtubule–kinesin contacts and the bent microneedle were balanced. This force balance clearly indicates that the microneedle is bent by the ATP-dependent active sliding force generated by the kinesin molecules interacting with the microtubules. The maximum 'isometric force' ($P_0$) attained by the kinesin molecules on the needle ranged from 2.4 to 7.9 pN (5.0±1.6 pN; mean ± S.D., $N$=24). As the bending portion of the microneedle was 2–3 mm long while the needle tip moved, at most, 10 $\mu$m, the resulting change in the needle tip angle with respect to the axoneme was negligible. The unidirectional needle movement was frequently interrupted by sudden detachment of the needle from the axoneme, resulting in large backward needle movements, and also by sudden stoppage of the needle movement.

In some cases, the kinesin-coated microneedle was also made to slide along the axoneme of a demembranated spermatozoon with its head attached. The needle always moved away from the sperm head. Since the plus-end of microtubules is located distal to the sperm head, this result

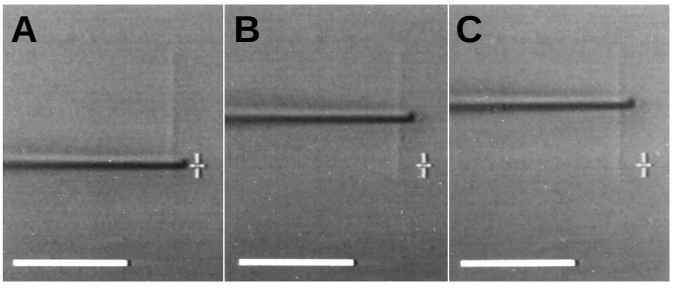


Fig. 2. Frames selected from a video tape showing sliding of the kinesin-coated tip of a microneedle along an axoneme placed at right angles to the needle. Frames B and C were taken 10 and 20 s, respectively, after frame A. The white cross in each frame indicates the initial position of the needle tip. Scale bar, 10 $\mu$m. Temperature, 23 °C.

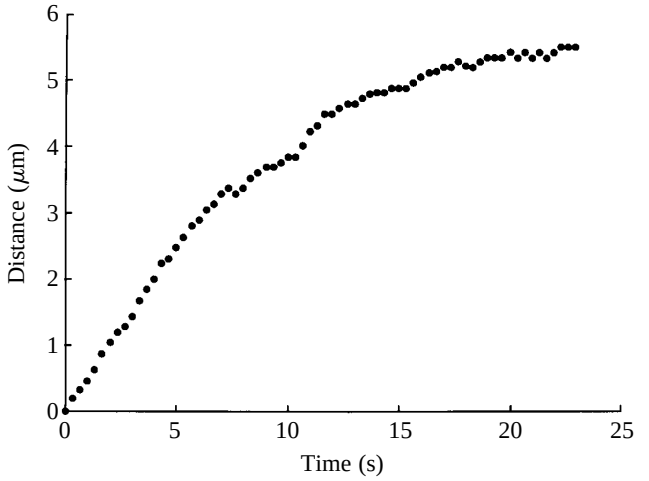


Fig. 3. A representative example of the time course of movement of a kinesin-coated microneedle along an axoneme at 24 °C.

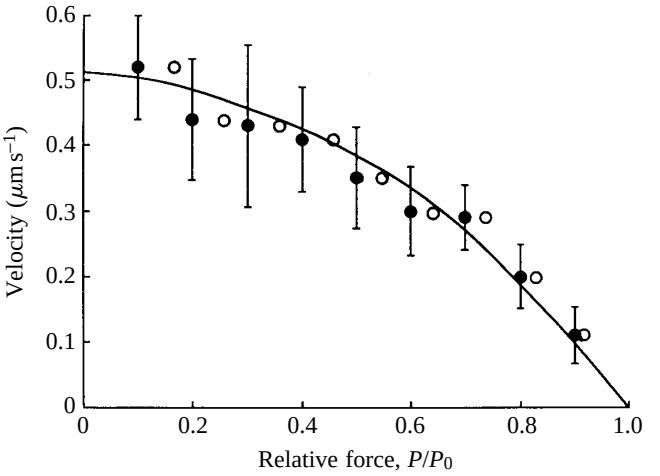


Fig. 4. Force–velocity relationship of microtubule–kinesin sliding, constructed from five different force–velocity data sets (filled circles). The amount of force (=load) is expressed relative to the maximum isometric force $P_0$ (mean, 6.4 pN). Data points represent mean values ± S.D. Data points corrected for the viscous drag force (see text) are also shown (open circles). The curve was drawn by eye. Temperature, 23–25 °C.

indicates, in agreement with a previous report (Vale *et al.* 1985), that the movement of the kinesin molecule along the microtubule is directed towards the plus end under the present experimental conditions.

*Time course of microneedle movement*

The time course of unidirectional microneedle movement was examined by determining the needle position on video frames taken at intervals of 333 ms. An example of the movement of the microneedle along the axoneme is shown in Fig. 3. The microneedle did not always progress smoothly along the axoneme, but showed irregular fluctuations in velocity. The needle movement records also contained short periods of backward movement (of less than 240 nm). Such velocity fluctuations have also been observed in kinesin-coated beads moving freely along a microtubule (Gelles *et al.* 1988) and may arise from factors such as local inhomogeneities of axoneme structure and fluctuations in the number of kinesin molecules responsible for the needle movement.

*Relationship between the force and velocity of needle movement*

Since the force on a microneedle could be calculated at any time from its displacement and elastic coefficient, the relationship between the force and the velocity of sliding between the kinesin molecules on the needle and the axoneme was examined under the auxotonic condition, i.e. the condition in which the load on the kinesin microtubule contact produced by the bent needle increased as needle movement progressed. Assuming that needle movement fluctuates around a smooth curve relating force and velocity, we determined the average velocities of needle movement for periods of 333 ms, under ten different loads equal to ten integral fractions of $P_0$ ($0.1P_0$, $0.2P_0$, etc.) from the slope of a straight line connecting the two end data points in each time period. The velocity measurements were carried out using only needle movement records in which relatively small velocity fluctuations occurred.

Fig. 4 shows the force–velocity relationship for microtubule–kinesin sliding in the auxotonic condition (filled circles) constructed from five different sets of force–velocity data (range of $P_0$, 2.4–7.9 pN; mean, 6.4 pN). The shape of the force–velocity curve was upwardly convex, as has been shown for the force–velocity curve of *in vitro* actin–myosin sliding in the auxotonic condition (Chaen *et al.* 1989). The maximum velocity of microtubule–kinesin sliding was 0.58±0.15 $\mu m\,s^{-1}$ (mean ± S.D., $N$=24), a value similar to those previously reported (0.5–0.6 $\mu m\,s^{-1}$, Vale *et al.* 1985; Gelles *et al.* 1988; Howard *et al.* 1989).

The viscous drag force on the moving microneedle was estimated in the following way. The microneedle tip was detached from the axoneme with a small horizontal displacement to keep its geometrical condition relative to the experimental chamber unchanged. The needle tip was then bent horizontally by 1–3 $\mu m$ using another rigid glass needle, and the needle tip was then suddenly released to restore its original position. The needle tip displacement $x$ (assuming negligible inertial forces) (in $\mu m$) is given by:

$$x = A[1 - \exp(-Kt/\zeta)],$$

where $A$ is the initial tip displacement of the bent needle (in $\mu m$), $K$ is the elastic coefficient (in pN $\mu m^{-1}$) of the needle, $t$ is time (in s) and $\zeta$ is the viscous drag coefficient (in pN $\mu m^{-1}$). Thus, the value of $\zeta$ can be determined from the time constant of the needle motion. In three needles examined, the time constant of needle motion was around 400 ms and the viscous drag coefficient was about 0.8 pN s $\mu m^{-1}$. For a microneedle moving at 0.5 $\mu m\,s^{-1}$, the viscous drag force is estimated to be 0.4 pN. This value amounts to less than 10 % of the $P_0$ values constituting the force–velocity curve in Fig. 4. Data points

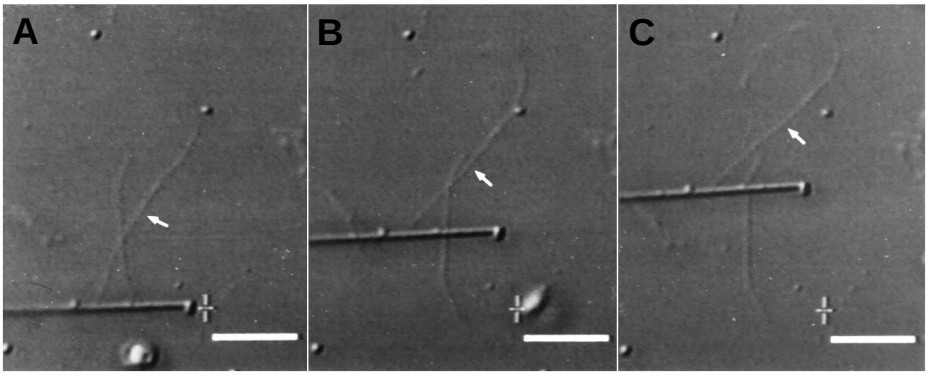


Fig. 5. Frames selected from a video tape showing the movement of an axoneme attached to a glass microneedle (indicated by an arrow in each frame) on the kinesin-coated glass surface. Frames B and C were taken 60 and 180 s, respectively, after frame A. The white cross in each frame indicates the initial position of the needle tip. Scale bar, 10 $\mu$m. Temperature, 23 °C.

corrected for the viscous drag force are also shown in Fig. 4 (open circles).

### *Movement of the axoneme attached to a microneedle on the kinesin-coated glass surface*

#### *Gradual change in shape of the axoneme following its contact with the kinesin-coated glass surface*

Frames selected from a video tape showing the movement of an axoneme, attached to the distal portion of a microneedle, on the kinesin-coated glass surface are shown in Fig. 5. For technical reasons, the axoneme was initially 'wavy' in shape when it was brought into contact with the glass surface (Fig. 5A), but then gradually became straight (in about 30 s, Fig. 5B) to continue its unidirectional movement on the kinesin molecules on the glass surface (Fig. 5C), until it eventually stopped moving after 30–100 s as a result of a balance between forces generated by the microtubule–kinesin contacts and the bent microneedle. Fig. 6 shows the change in shape of the axoneme over six frames following its contact with the glass surface. As the axis of the straightened axoneme was not oriented at right angles to the microneedle axis, the axoneme moved obliquely on the glass surface, while generating the force to bend the needle (Fig. 5B,C). The axoneme was attached to the needle so firmly that it never became detached during repeated sliding on the kinesin-coated glass surface.

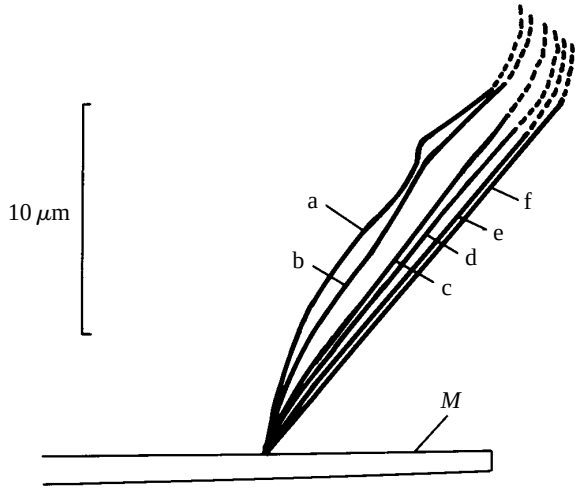


Fig. 6. Change in shape of the axoneme attached to a glass microneedle (*M*), sliding on the kinesin-coated glass surface. Traces b–f show the shape of the axoneme 5, 10, 15, 20 and 25 s, respectively, after trace a. In each trace, the broken line indicates the part of the axoneme which is obviously not in contact with the kinesin-coated glass surface. The traces were obtained from the video tape shown in Fig. 5.

#### *Time course of the axoneme movement*

As shown in Fig. 7, the time course of the resulting microneedle movement (Fig. 7) was analogous to that of the kinesin-coated microneedle on the axoneme and also showed irregular fluctuations in the velocity of movement. It was noted that the irregular fluctuations became more obvious after the axoneme had straightened, indicating that axoneme straightening was associated with relatively smooth needle movement. The maximum velocity of microneedle movement was 0.68±0.17 $\mu$m s$^{-1}$ (mean ± S.D., $N$=6), while the maximum force exerted by the bent needle was 46.1±18.6 pN ($N$=6). We did not construct force–velocity curves from the needle movement records, because the sliding between the axoneme attached to the needle and the kinesin-coated glass surface was much more complicated than the sliding between the kinesin-coated needle and the axoneme, in which the same kinesin

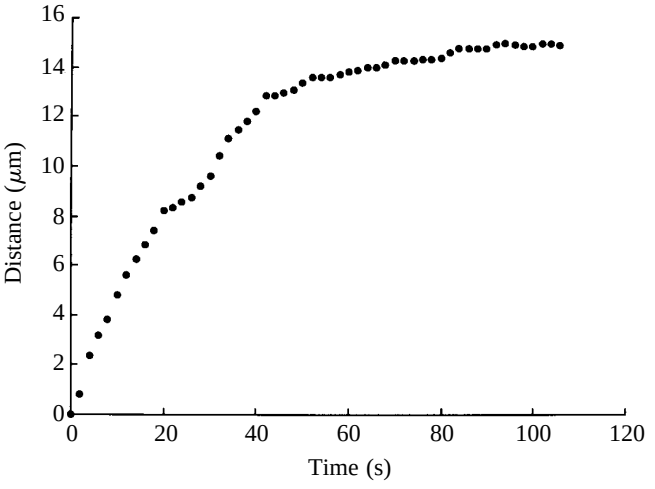


Fig. 7. A representative example of the time course of movement of the microneedle to which the axoneme sliding on the kinesin-coated glass surface is attached. Temperature, 25 °C.

molecules could interact with microtubules during the whole period of auxotonic sliding.

## Discussion

### *Comparison of kinetic properties between microtubule–kinesin and actin–myosin sliding*

Using the *in vitro* assay system in which a kinesin-coated microneedle is made to slide along an axoneme (Figs 1A, 2), we have obtained a convex force–velocity relationship for microtubule–kinesin sliding in the auxotonic condition (Fig. 4). Analogous convex force–velocity curves have also been obtained in the auxotonic condition for *in vitro* sliding of a myosin-coated microneedle along actin cables in giant algal cells (Chaen *et al.* 1989) and also for the auxotonic shortening of intact frog skeletal muscle fibres (Iwamoto *et al.* 1990).

Iwamoto *et al.* (1990) have shown that the convex shape of the force–velocity curves of muscle fibres in the auxotonic condition can be accounted for using two simplified assumptions within the framework of the Huxley contraction model (Huxley, 1957): (1) the rate constant for the breaking of actin–myosin linkages increases as the velocity of actin–myosin sliding increases and (2) the average force generated by an actin–myosin linkage decreases as the velocity of actin–myosin sliding increases. This suggests that the above kinetic properties of actin–myosin sliding may also hold for microtubule–kinesin sliding, although more experimental work is needed to clarify this point.

In the present study, the kinesin-coated needles could slide along the axoneme over many micrometres (2–10 $\mu$m) with $P_0$ values ranging from 2.4 to 7.9 pN (Fig. 3), indicating that such long sliding distances can be achieved by a small number of kinesin molecules. In contrast, myosin-coated needles tend to become detached from actin cables when the number of myosin molecules involved in needle movement is reduced to less than 40 (Oiwa *et al.* 1993). These results are consistent with the view that the time at which kinesin is detached from microtubules in a microtubule–kinesin ATPase cycle is very short compared with the time at which myosin becomes detached from actin in an actin–myosin ATPase cycle (Howard *et al.* 1989; Block *et al.* 1990; Romberg and Vale, 1993).

### *Comparison of the present results with other work*

Several authors have estimated values for the maximum isometric force generated by a single kinesin molecule, with diverse results (0.12±0.03 pN, Hall *et al.* 1993; 1.9±0.4 pN, Kuo and Sheetz, 1993; 5.7±0.4 pN, Svoboda and Block, 1994; 4.2±0.5 pN, Hunt *et al.* 1994). This diversity may result partly from the different techniques used [centrifuge microscope (Hall *et al.* 1993), optical trap (Kuo and Sheetz, 1993; Svoboda and Block, 1994) and viscous load (Hunt *et al.* 1994)] and partly from different experimental conditions, including the calibration of measurements, the orientation of the kinesin molecules relative to the microtubules and the uncertainty of recording the response of a single kinesin molecule. Although it was not our intention to measure the force of a single kinesin molecule, the minimum value of $P_0$ obtained in the present work (2.4 pN), which might be generated by a single kinesin molecule, falls within the reported range for a single kinesin molecule.

Recently, Svoboda and Block (1994) constructed a force–velocity relationship for the sliding of kinesin-coated beads on microtubules within an optical trap imposing an auxotonic load on microtubule–kinesin sliding. In an optical trap, the beads moved for a limited distance (usually less than 200 nm), until the kinesin force balanced the trap force, and were then suddenly detached to return to the position with zero trapping force and, after some period, resumed sliding. Such ‘back-and-forth’ bead movement took place many times. For each forward bead movement, the velocities of bead movement along the noisy movement trace were measured, and averaged velocities for each fraction of auxotonic load were obtained. Despite their claim that they were observing the behaviour of single kinesin molecules, inspection of typical records indicates that the maximum force of a single kinesin molecule varied between records by a factor of 2, while the time at which the force of a single kinesin molecule reached a maximum within the same trap varied by a factor of more than 10. As a result, the force–velocity plot exhibited considerable scatter of data points, which suggests that different numbers of kinesin molecules with differing orientation were brought into contact with microtubules during the repeated bead sliding movement and that both the velocity of microtubule–kinesin sliding and the maximum kinesin force attained depended markedly on the mode of kinesin–microtubule contact.

In the present study, however, the bead surface with which kinesin molecules interact with microtubules was kept virtually constant throughout bead movement extending over many micrometres and, therefore, our data points were likely to have been obtained from the same kinesin molecules sliding along the microtubules. The present force–velocity curve for microtubule–kinesin sliding (Fig. 4) may more accurately reflect what actually takes place when a few kinesin molecules transport cellular components in living cells than the force–velocity data obtained previously (Svoboda and Block, 1994; Hunt *et al.* 1994). The present results do not, however, give information about whether the force–velocity relationship is associated with any change in the number or in the mode of operation of the kinesin molecules involved. It should be noted that the same situation also holds for the force–velocity relationship of actin–myosin sliding in contracting muscle. Much more experimental work is needed to elucidate the mechanism underlying the force–velocity relationship in both actin–myosin and microtubule–kinesin sliding.

### *Flexibility of kinesin molecules*

When an axoneme attached to a microneedle was brought into contact with the glass surface, it was wavy in shape, but it then became gradually straightened during the progress of microtubule–kinesin sliding (Figs 5, 6), so that the force generated by the kinesin molecules interacting with the axoneme could sum additively along the long axis of the

axoneme to oppose the force exerted by the bent needle. As the straightened axoneme was not parallel with the direction of needle movement, the axoneme moved at an oblique angle to its long axis while pulling the needle to which it was attached (Figs 5, 6). Since the kinesin molecules are randomly oriented on the glass surface, the oblique axoneme movement indicates an enormous flexibility of kinesin molecules in adjusting their direction of force generation to the long axis of the axoneme. If each kinesin molecule had no such flexibility, the axoneme might not be able to interact with suitable kinesin molecules to move the needle obliquely over a large distance. Hall *et al.* (1993) studied the force–velocity relationship of a sea-urchin spermatozoon sliding on a kinesin-coated glass surface in the isotonic condition using a centrifuge microscope. As the kinesin molecules were randomly oriented on the glass surface, the feasibility of such experiments is obviously based on the flexibility of kinesin molecules, which allows them to adjust their direction of force generation to that of the centrifugal force.

## References


BELL, C. W., FRASER, C., SALE, W. A., TANG, W. J. Y. AND GIBBONS, I. R. (1982). Preparation and purification of dynein. In *Methods in Cell Biology*, vol. 24 (ed. L. Wilson), pp. 373–397. New York: Academic Press.

BLOCK, S. M., GOLDSTEIN, L. S. B. AND SCHNAPP, B. J. (1990). Bead movement by single kinesin molecules studied with optical tweezers. *Nature* **348**, 348–352.

BRADFORD, M. M. (1976). A rapid and sensitive method for the quantitation of microgram quantities of protein utilizing the principle of protein–dye binding. *Analyt. Biochem.* **72**, 248–254.

CHAEN, S., OIWA, K., SHIMMEN, T., IWAMOTO, H. AND SUGI, H. (1989). Simultaneous recordings of force and sliding movement between a myosin-coated glass microneedle and actin cables *in vitro*. *Proc. natn. Acad. Sci. U.S.A.* **86**, 1510–1514.

GELLES, J., SCHNAPP, B. J. AND SHEETZ, M. P. (1988). Tracking kinesin driven movement with nanometre-scale precision. *Nature* **331**, 450–453.

HALL, K., COLE, D. G., YEH, Y., SCHOLEY, J. M. AND BASKIN, R. J. (1993). Force–velocity relationships in kinesin-driven motility. *Nature* **364**, 457–459.

HOWARD, J., HUDSPETH, A. J. AND VALE, R. D. (1989). Movement of microtubules by single kinesin molecules. *Nature* **342**, 154–158.

HUNT, A. J., GITTES, F. AND HOWARD, J. (1994). The force exerted by a single kinesin molecule against a viscous load. *Biophys. J.* **67**, 766–781.

HUXLEY, A. F. (1957). Muscle structure and theories of contraction. *Prog. Biophys. biophys. Chem.* **7**, 136–195.

IWAMOTO, H., SUGAYA, R. AND SUGI, H. (1990). Force–velocity relation of frog skeletal muscle fibres shortening under continuously changing load. *J. Physiol., Lond.* **422**, 185–202.

KUO, S. C. AND SHEETZ, M. P. (1993). Force of single kinesin molecules measured with optical tweezers. *Science* **260**, 232–234.

OIWA, K., CHAEN, S., KAMITSUBO, E., SHIMMEN, T. AND SUGI, H. (1990). Steady-state force–velocity relation in the ATP-dependent sliding movement of myosin-coated beads on actin cables *in vitro* studied with a centrifuge microscope. *Proc. natn. Acad. Sci. U.S.A.* **87**, 7893–7897.

OIWA, K., KAWAKAMI, T. AND SUGI, H. (1993). Unitary distance of actin–myosin sliding studied using an *in vitro* force–movement assay system combined with ATP iontophoresis. *J. Biochem., Tokyo* **114**, 28–32.

ROMBERG, L. AND VALE, R. D. (1993). Chemomechanical cycle of kinesin differs from that of myosin. *Nature* **361**, 168–170.

SHIMIZU, T., FURUSAWA, K., OHASHI, S., TOYOSHIMA, Y. Y., OKUNO, M., MALIK, F. AND VALE, R. D. (1991). Nucleotide specificity of the enzymatic and motile activities of dynein, kinesin and heavy meromyosin. *J. Cell Biol.* **112**, 1189–1197.

SVOBODA, K. AND BLOCK, S. M. (1994). Force and velocity measured for single kinesin molecules. *Cell* **77**, 773–784.

VALE, R. D., SCHNAPP, B. J., MITCHSON, T., STEUER, E., REESE, T. S. AND SHEETZ, M. P. (1985). Different axoplasmic proteins generate movement in opposite directions along microtubules *in vitro*. *Cell* **43**, 623–632.

YONEDA, M. (1960). Force exerted by a single cilium of *Mytilus edulis*. *J. exp. Biol.* **37**, 461–468.